

Basics of RF superconductivity

Walter Venturini Delsolaro
CERN

Lectures for the CERN summer students,
14-15 July 2021

Outline- part 2

- Superconducting cavity technologies
 - RF acceleration vs particle velocity
 - cavity design
 - SRF materials: Pb, bulk Nb, Nb₃Sn, Nb/Cu
 - RF surface engineering: chemical polishing, EP, baking, N-doping, multilayers
 - Cavity testing
 - Cavity performance: accelerating fields, cryogenics losses, detuning effects
 - Classical cavity limitations: Global thermal instability, Q disease, multipacting, field emission
 - Field dependent surface resistance

Acknowledgement

- A lot of excellent introductory material can be found online in the tutorials of the SRF workshop and in previous CERN training courses.
- Big thanks to S. Belomestnykh, G. Ciovati, E. Jensen, A. Myasaki, R. Vaglio

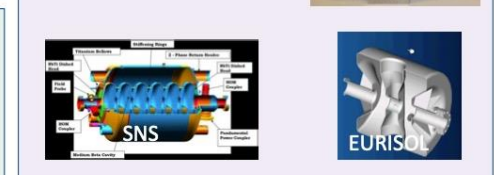
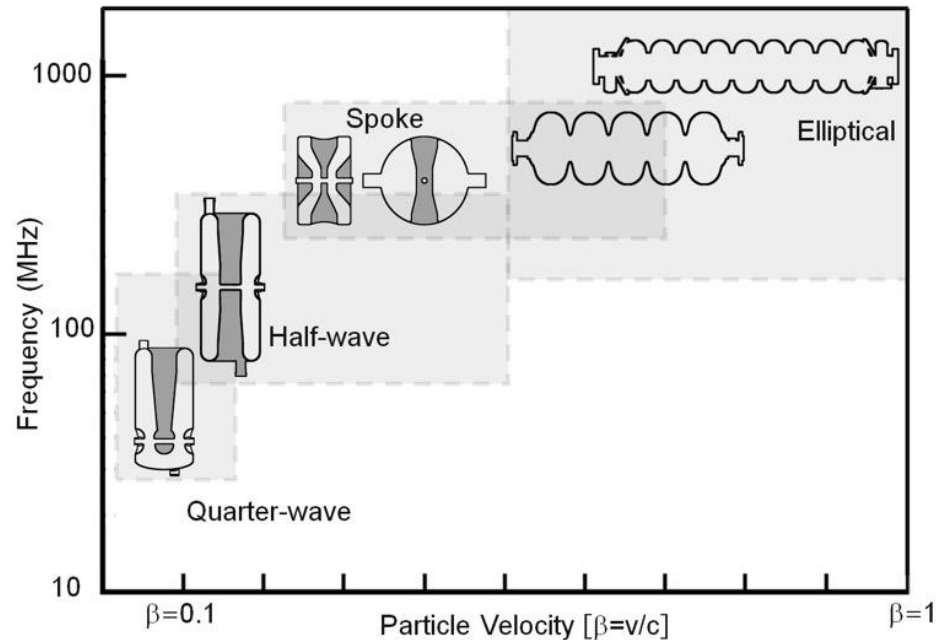
Types of SRF accelerating structures

Three groups: low, medium and high β structures. The accelerating gap length is typically $\frac{\beta\lambda}{2}$ where λ is the wavelength of the e.m. field

For ultra relativistic particles ($\beta \sim 1$) elliptical multi cells operating in the TM010 resonant mode and high (GHz) frequency are used: compact, maximize real estate gradient

Elliptical shapes start to be mechanically unstable for $\beta \sim 0.5$. Also, lower frequencies are favoured for protons and ions: elliptical shapes become large and other solutions become competitive

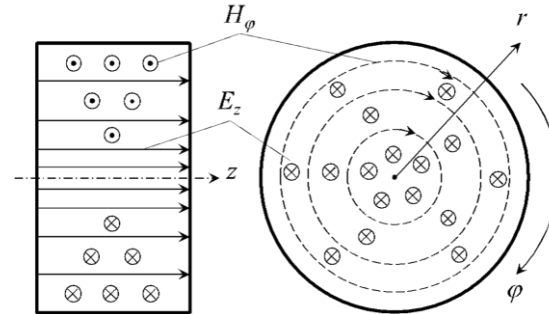
For particles moving at small fractions of c , low frequency is needed to provide sufficient acceleration during the transit in the cavity (see later)



RF design

- Solve Maxwell equations in closed domain with perfectly conducting boundary walls

$$\begin{cases} \left(\nabla^2 - \frac{1}{c^2} \frac{\partial^2}{\partial t^2} \right) \begin{Bmatrix} \mathbf{E} \\ \mathbf{H} \end{Bmatrix} = 0 \\ n \times \mathbf{E} = 0, n \cdot \mathbf{H} = 0 \end{cases}$$



- Analytical solutions exist only for a few simple geometries (sphere, cylinders) with high symmetry, for example the pill box
- In general, solutions can be classified into families of modes with different field pattern and eigenfrequencies: TE modes have only transverse electric fields; TM modes have only transverse magnetic fields.
- For the pill box, the fields and the resonant frequency of the TM₀₁₀ mode are:

$$E_z = E_0 J_0 \left(\frac{2.405 r}{R} \right) e^{i\omega t}, \quad H_\varphi = -i \frac{E_0}{\eta} J_1 \left(\frac{2.405 r}{R} \right) e^{i\omega t}, \quad \eta = \sqrt{\frac{\mu_0}{\epsilon_0}}, \quad \omega_0 = \frac{2.405 c}{R}$$

- One mode is used for acceleration (in elliptical structures this is the TM₀₁₀)
- The other modes are unwanted (but always present): if excited can have a detrimental effect on the beam dynamics
- Real cavities shapes have to be simulated with numerical codes

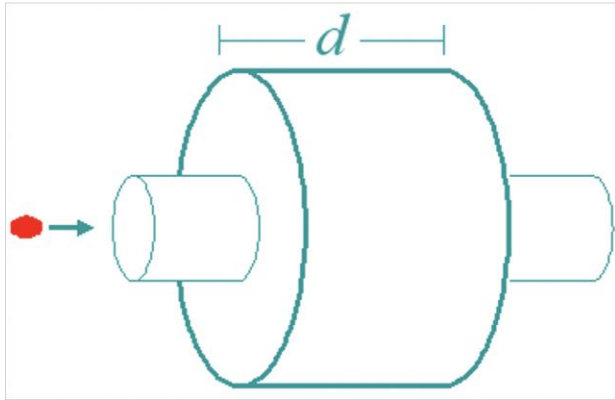
Quality factor

$$Q = \frac{2\pi (\text{Energy stored per cycle})}{\text{Energy dissipated per cycle}}$$

$$Q = \frac{\omega_0 \mu_0 \iiint H^2 dv}{R_s \iint H^2 ds} = \frac{\Gamma}{R_s}$$

Assuming that the surface resistance R_s does not vary over the cavity surface and has no field dependence.

Cavity voltage and transit time factor



The voltage experienced by a charged particle travelling along the cavity axis is

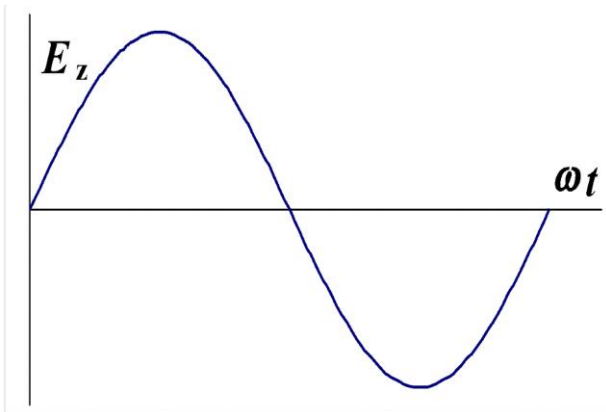
$$V_c = \int_{-\infty}^{+\infty} E_z(r=0, z) e^{\frac{i\omega z}{\beta c}} dz$$

For the pill box, the integral can be computed analytically, yielding

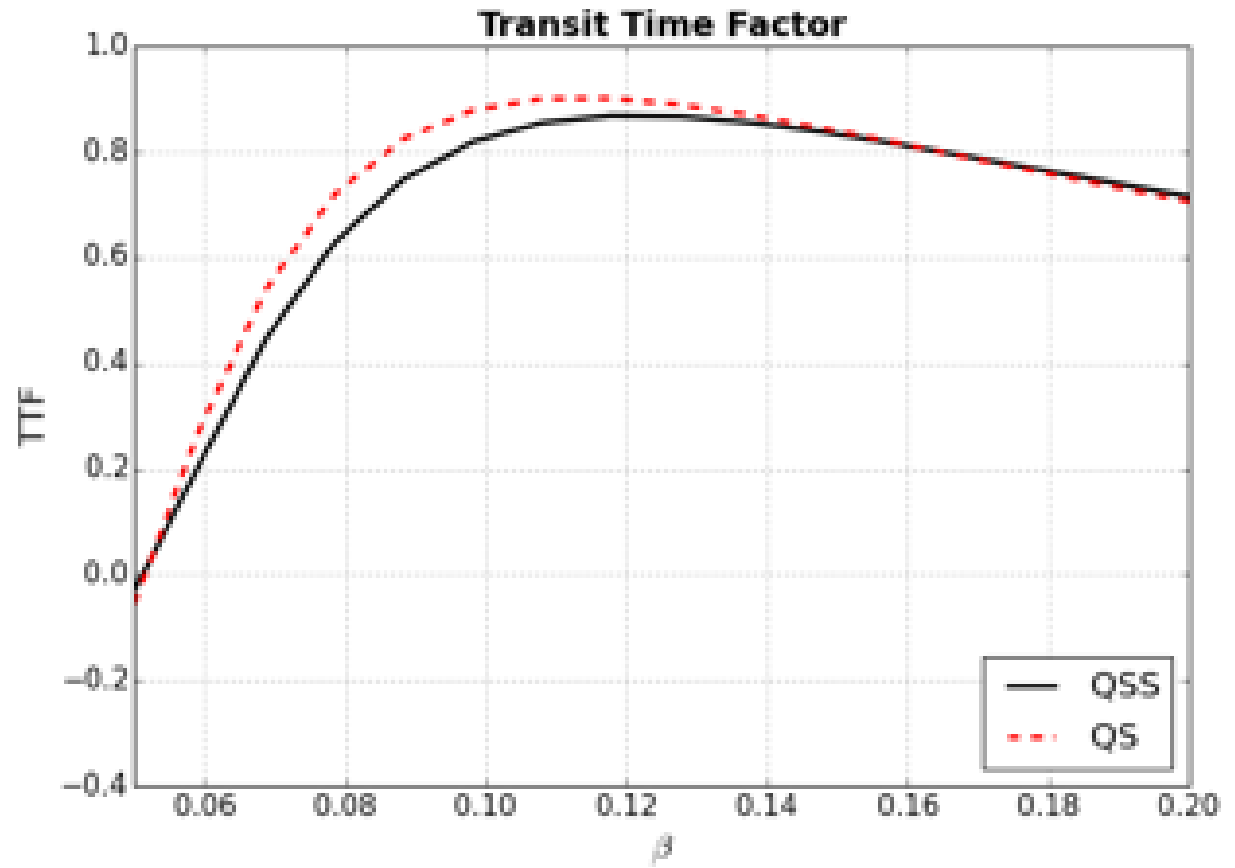
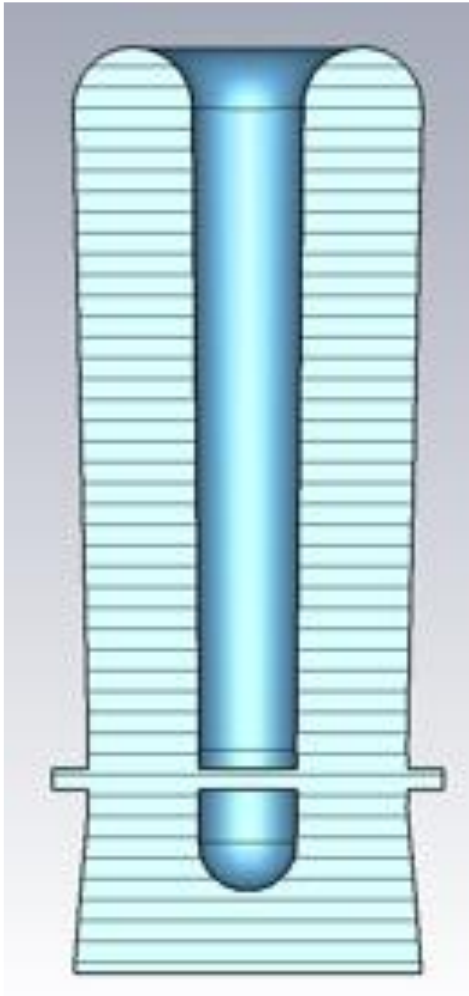
$$V_c = \int_0^d e^{\frac{i\omega z}{\beta c}} dz = E_0 d \frac{\sin\left(\frac{\omega_0 d}{2\beta c}\right)}{\frac{\omega_0 d}{2\beta c}}$$

The accelerating field can be defined as

$$E_a = \frac{V_c}{d}$$



TTF(β) for two gap structure: example of HIE ISOLDE QWR



Shunt impedance

The shunt impedance is the parameter that defines the efficiency of the cavity to convert RF power to voltage gain or, in other words, the effective voltage for a given power dissipated on the cavity walls. It can be defined as

$$R = \frac{V_{\text{eff}}^2(\beta)}{P_c}.$$

Ideally, we want it to be large in order to minimize the power dissipation.

The ratio of shunt impedance and quality factor (R/Q) is a purely geometrical figure that is used as a figure of merit to quantify the efficiency of acceleration of a given structure:

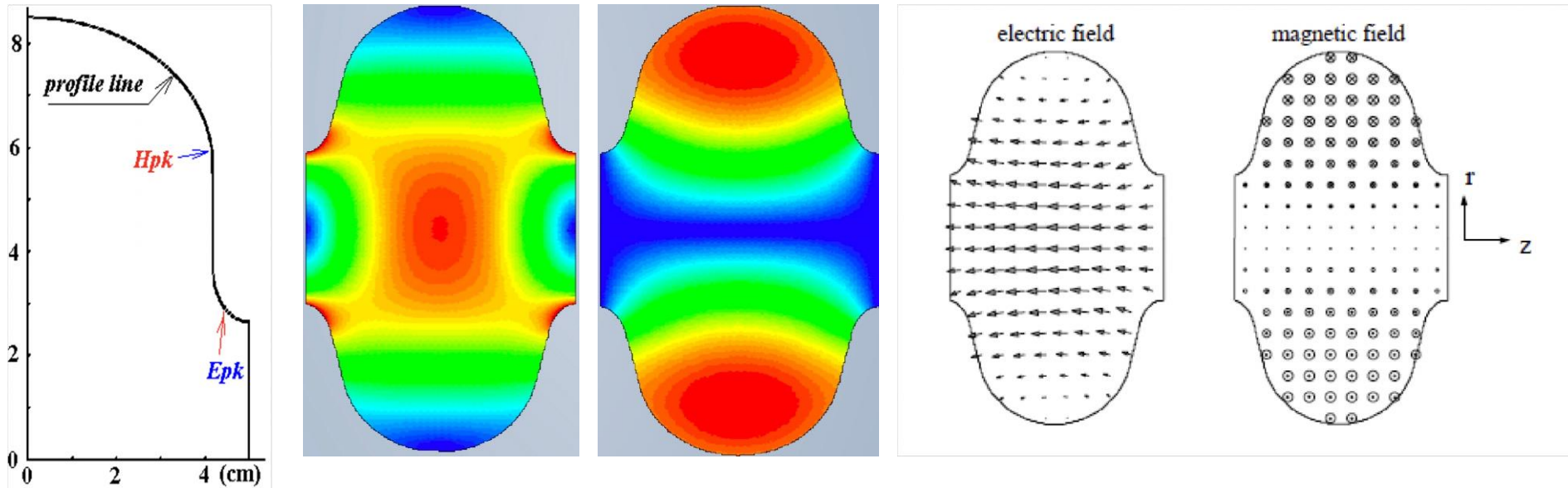
$$\frac{R}{Q_0} = \frac{V_{\text{eff}}^2}{\omega_0 U}$$

The dissipated power is then:

$$P_c = \frac{V_{\text{eff}}^2(\beta)}{\frac{R}{Q_0} Q_0},$$

factoring out the voltage, the R/Q and the quality factor.

Peak fields



Peak fields should be minimized relative to the accelerating field (minimize ratios)

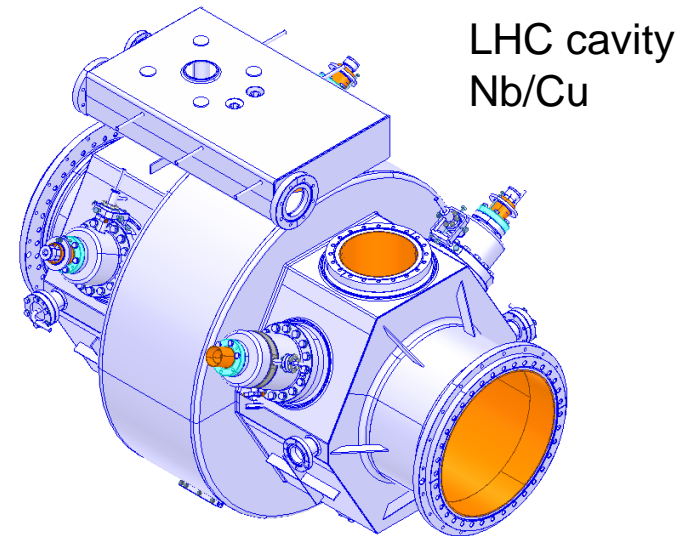
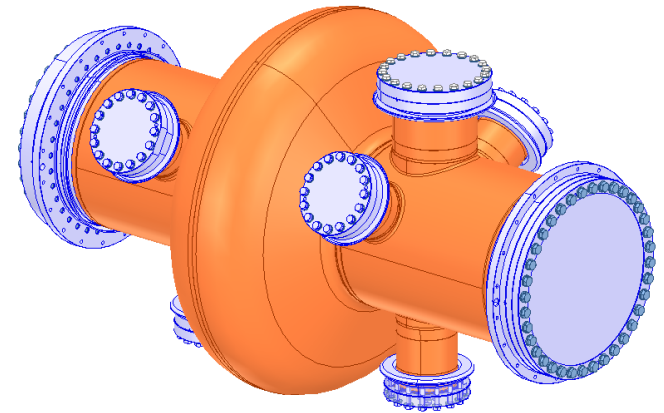
The magnetic field is responsible for losses and is limited in the superconducting state by critical fields

No known limitations on the electric field in a superconductor, but high E field will cause field emission for non ideal surfaces, which can severely limit the performance

Typical values of $\frac{E_{peak}}{E_{acc}}$ and of $\frac{B_{peak}}{E_{acc}}$ in elliptical structures: 2-2.6, and 4-5 mT/(MV/m)

Mechanical design

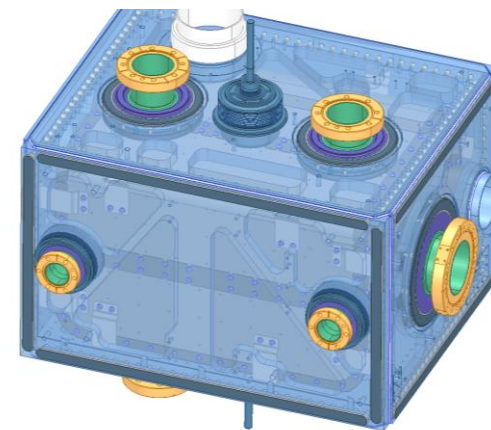
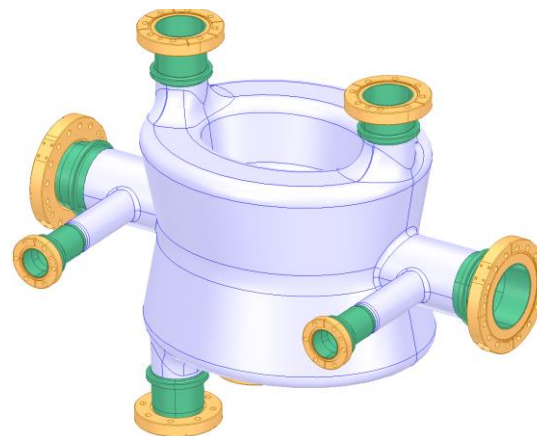
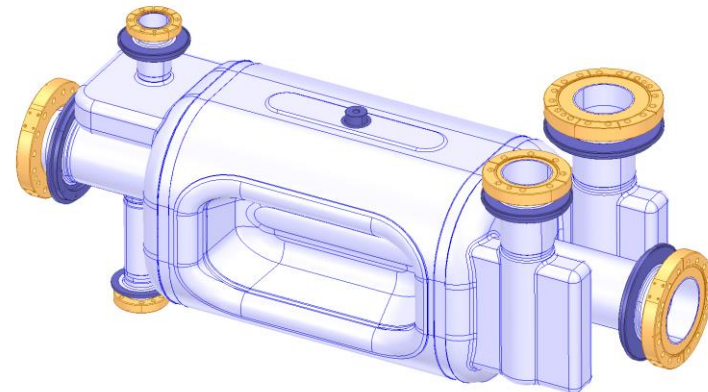
- Integration of RF input coupler ports, HOM coupler ports & field probes
- Definition of interfaces:
 - mechanical supports,
 - helium space,
 - beam vacuum
 - Instrumentation (T, p, B)
- Calculation (making use of different numerical codes) of:
 - mechanical stresses due to cooldown or pressure differences
 - Frequency shifts, tuning range
 - heat transfer
 - Mechanical vibrations modes (microphonics)
 - Lorentz force detuning



HL-LHC DQW & RFD crab cavities

- Bulk Nb cavity (RRR 300)
- Nb parts Electron beam welded
- 316LN flanges vacuum brazed
- Titanium bellows and NbTi interfaces
- Bolted titanium helium tank with magnetic shielding inside
- **1 FPC + 3 HOM couplers + 2 Pickups**

Parameters	DQW	RFD
Cavity thickness [mm]	4	
Beam aperture [mm]	84	
Cavity stiffness [kN/mm]	2.4	3.15
Tuning sensitivity [kHz/mm]	318	530
Tuning range at 2 K [mm]	± 1.6	± 2.45
Tuning range at 2 K [kHz]	± 509	± 1300
Lorentz force detuning coef [Hz/(MV ²)]	-400	-555
Pressure sensitivity [Hz/mbar]	780	-193
Operating pressure [barg]	0.8	
Maximum Allowable Working Pressure [barg]	1.1	



Cavity design/optimization

A complex optimization problem with many variables and objective functions: still room for creativity and fancy math...

PHYSICAL REVIEW ACCELERATORS AND BEAMS **22**, 122001 (2019)

Constrained multiobjective shape optimization of superconducting rf cavities considering robustness against geometric perturbations

Marija Kranjčević^{1,*}, Shahnam Gorgi Zadeh,² Andreas Adelman,³
Peter Arbenz,^{1,†} and Ursula van Rienen^{2,‡}

¹*Department of Computer Science, ETH Zurich, 8092 Zürich, Switzerland*

²*Institute of General Electrical Engineering, University of Rostock, 18059 Rostock, Germany*

³*Paul Scherrer Institut (PSI), 5232 Villigen, Switzerland*



(Received 31 May 2019; published 23 December 2019)

High current storage rings, such as the Z-pole operating mode of the FCC-ee, require accelerating cavities that are optimized with respect to both the fundamental mode and the higher order modes. Furthermore, the cavity shape needs to be robust against geometric perturbations which could, for example, arise from manufacturing inaccuracies or harsh operating conditions at cryogenic temperatures. This leads to a constrained multiobjective shape optimization problem which is computationally expensive even for axisymmetric cavity shapes. In order to decrease the computation cost, a global sensitivity analysis is performed and its results are used to reduce the search space and redefine the objective functions. A massively parallel implementation of an evolutionary algorithm, combined with a fast axisymmetric Maxwell eigensolver and a frequency-tuning method is used to find an approximation of the Pareto front. The computed Pareto front approximation and a cavity shape with desired properties are shown. Further, the approach is generalized and applied to another type of cavity.

Choice of the raw material: the ideal SRF material should provide:

- Low surface resistance, including low residual resistance at $T \rightarrow 0$;
- An s-wave Cooper pairing state with a full superconducting gap on the entire Fermi surface;
- A high lower critical magnetic field H_{c1} at which the weakly dissipative Meissner state is destroyed due to penetration of vortices;
- A high superheating magnetic field which defines the theoretical limit of the SRF breakdown;
- High thermal conductivity to transfer the rf dissipated power through the cavity wall;
- Grain boundaries transparent to high rf screening currents in polycrystalline cavities;
- Comparatively simple chemical composition, so that the material is not contaminated by non-superconducting second phases, and the superconducting properties are not degraded by local nonstoichiometry;
- Good mechanical properties and malleability to minimize crack formation during cavity manufacturing (forging, deep drawing, etc.)

RF superconductors

	Type	T_c	B_{c1}	B_c	B_{c2}	Form
		K	mT	mT	mT	
Nb	II	9.25	170	206	400	bulk, film
Pb	I	7.20	-	80	-	film
Nb ₃ Sn	II	18.1	38	520	24000	film

- The list is short... lead used to be electroplated on copper, was superseded by Nb due to the field limitation, but could still be useful in some applications
- Nb is the « workhorse » either in bulk form or as a thin layer deposited on the inner surface of a copper structure
- Alloys are “dirty” superconductors due to their small mean free path, they are usually brittle and poor thermal conductors.
- High T_c superconductors showed very high surface resistances: low coherence length → sensitivity to defects, premature flux entry, low B_{c1} , gap anisotropy.
- Nb₃Sn (and other compounds of the A15 family) are attractive for 4.2 K operation, field limitations are not clear. So far 25 MV/m was the maximum reached.

SRF cavity manufacturing steps

- Mainstream technology is based on bulk Nb sheets formed and electron beam welded to create the resonators
- High purity is not optimal for SRF (remember R_{BCS} vs m.f.p)
- High purity (RRR) Nb is required for thermal conductivity
- EB welding to preserve material purity over the joining steps
- Detailed manufacturing process depends on cavity shape
- RF surface is obtained by means of chemical/electrochemical and thermal treatments to remove damage layers , smoothen the surface, and tune the properties of the RF layer
- Final surface must be free of particulate (dust) to avoid field emission
- Work in clean room and ultra pure water rinsing at high pressure to prepare the surface for test or operation

Nb purification

PERIODIC TABLE OF ELEMENTS

1 H Hydrogen																
3 Li Lithium	4 Be Beryllium											5 B Boron	6 C Carbon	7 N Nitrogen	8	
11 Na Sodium	12 Mg Magnesium											13 Al Aluminium	14 Si Silicon	15 P Phosphorus	16	
19 K Potassium	20 Ca Calcium	21 Sc Scandium	22 Ti Titanium	23 V Vanadium	24 Cr Chromium	25 Mn Manganese	26 Fe Iron	27 Co Cobalt	28 Ni Nickel	29 Cu Copper	30 Zn Zinc	31 Ga Gallium	32 Ge Germanium	33 As Arsenic	34	
37 Rb Rubidium	38 Sr Strontium	39 Y Yttrium	40 Zr Zirconium	41 Nb Niobium	42 Mo Molybdenum	43 Tc Technetium	44 Ru Ruthenium	45 Rh Rhodium	46 Pd Palladium	47 Ag Silver	48 Cd Cadmium	49 In Indium	50 Sn Tin	51 Sb Antimony	52	
55 Cs Caesium	56 Ba Barium	57 La* Lanthanum	72 Hf Hafnium	73 Ta Tantalum	74 W Tungsten	75 Re Rhenium	76 Os Osmium	77 Ir Iridium	78 Pt Platinum	79 Au Gold	80 Hg Mercury	81 Tl Thallium	82 Pb Lead	83 Bi Bismuth	84	
87 Fr Francium	88 Ra Radium	89 Ac** Actinium	104 Rf Rutherfordium	105 Db Dubnium	106 Sg Seaborgium	107 Bh Bohrium	108 Hs Hassium	109 Mt Meitnerium	110 Ds Darmstadtium	111 Rg Roentgenium	112 Cn Copernicium	113 Nh Nihonium	114 Fl Flerovium	115 Mc Moscovium	116	

* 58 Ce Cerium	59 Pr Praseodymium	60 Nd Neodymium	61 Pm Promethium	62 Sm Samarium	63 Eu Europium	64 Gd Gadolinium	65 Tb Terbium	66 Dy Dysprosium	67 Ho Holmium	68 Er Erbium	69 Tm Thulium	70 Yb Ytterbium
** 90 Th Thorium	91 Pa Protactinium	92 U Uranium	93 Np Neptunium	94 Pu Plutonium	95 Am Americium	96 Cm Curium	97 Bk Berkelium	98 Cf Californium	99 Es Einsteinium	100 Fm Fermium	101 Md Mendelevium	102 No Nobelium



Niobe



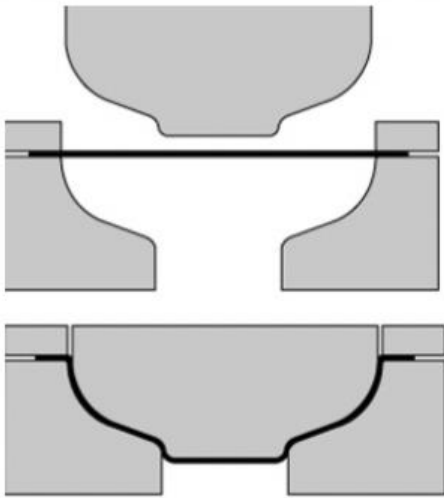
Tantalus

Cavity grade Nb chemical composition

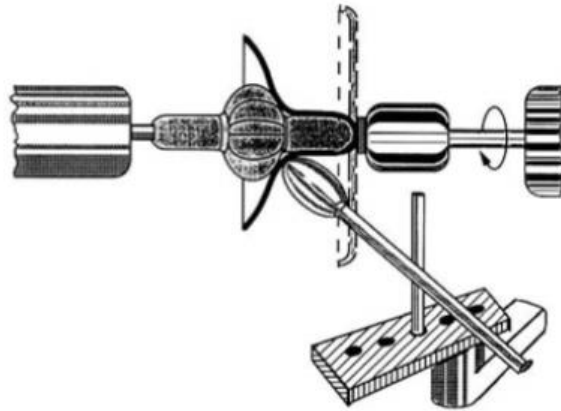
S. No	Impurities	Limiting Value
•		High RRR Niobium
		Blank and Sheet
1	H	≤ 5 ppm
2	N	≤ 30 ppm
3	O	≤ 40 ppm
4	C	≤ 30 ppm
5	Ta	≤ 1000 ppm
6	Ti	≤ 50 ppm
7	W	≤ 70 ppm
8	Fe	≤ 50 ppm
9	Si	≤ 50 ppm
10	Mo	≤ 30 ppm
11	Ni	≤ 70 ppm
12	Any other (Individually)	≤ 50 ppm

Forming techniques

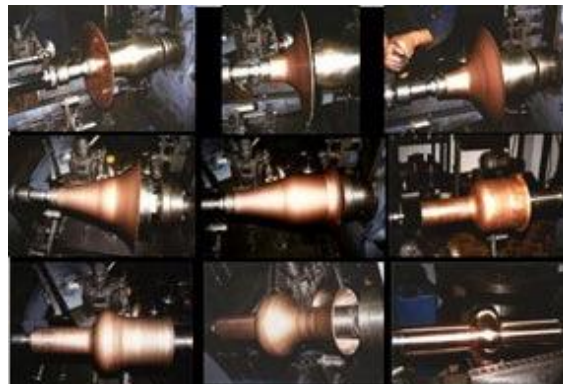
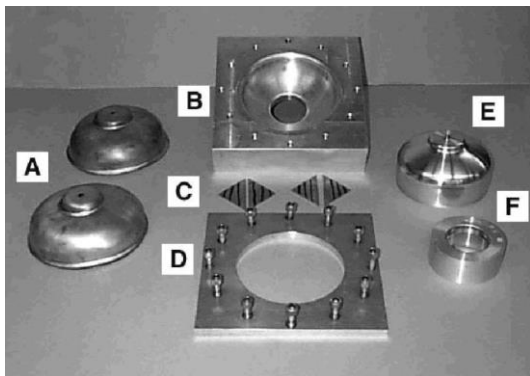
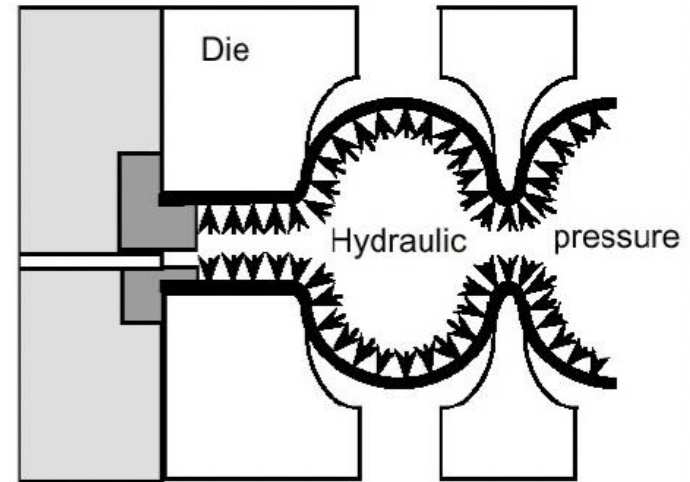
Deep drawing



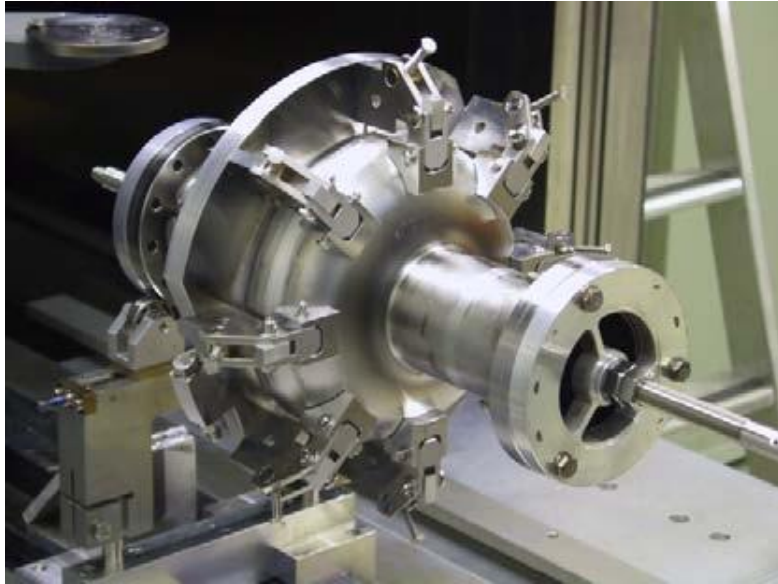
Spinning/ flow turning



Hydroforming



EB welding



From “1.3 GHz Niobium Single-Cell Fabrication Sequence” , DESY- TTC Report 2010-01



Welds on Quadrupole resonator pole shoes at CERN

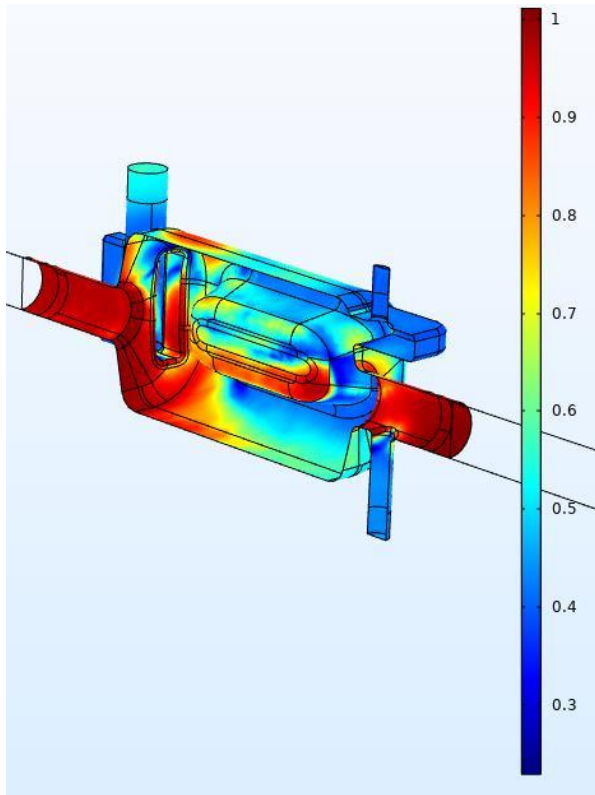


Welding of CRAB cavities at CERN

Nb Buffered Chemical Polishing

Nb etching by means of a mixture of HF, HNO₃ and H₃PO₄

Simpler to implement than EP, it can enhance roughness due to preferential etching of grains depending on crystal orientation

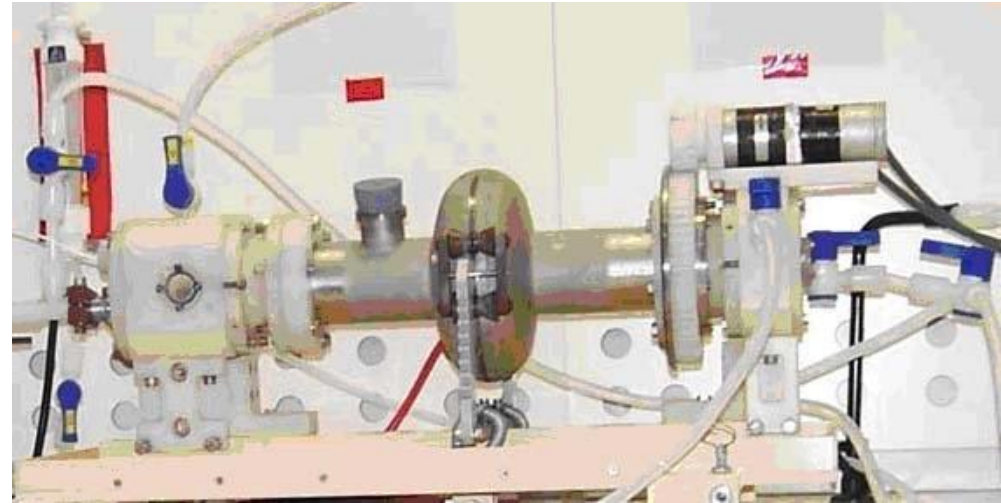
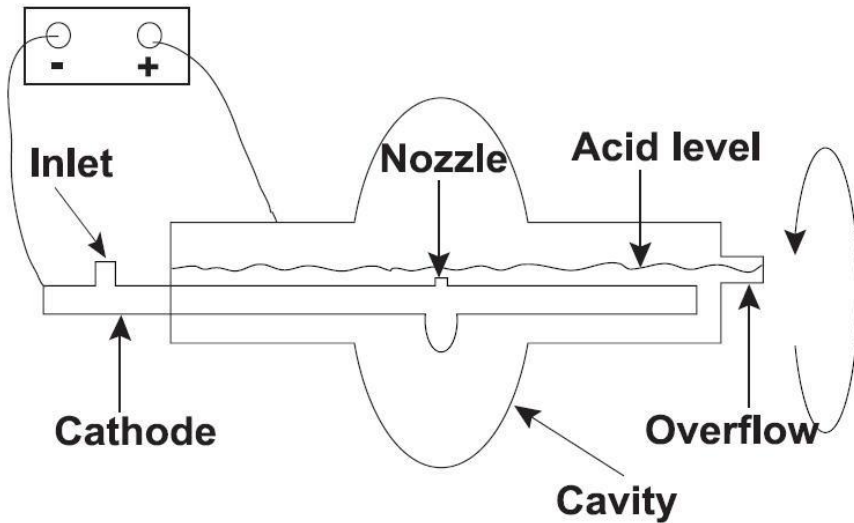


Multiphysics simulations of etching rate



BCP installations at CERN

Electro polishing (Nb)



The electrolyte is a mixture of hydrofluoric and sulfuric acid. The reaction proceeds in two steps:

- Oxidation of Nb to Nb pentoxide by the Sulfuric acid
- Dissolution of the pentoxide by the HF

Great care must be taken in controlling voltage, current density, temperature, acid flow rate, and electrolyte composition. Optimal working point in the I-V curve

High pressure water rinsing



Ultrapure water plant
Resistivity (25 °C) > 18 MΩ·cm



Rinsing cabinet

Another way to do it: Nb coating on copper

- RF currents don't flow in the bulk of the cavity wall: the London penetration depth for Nb is of ~ 40 nm
- Superconductors are bad thermal conductors (Cooper pairs do not transport entropy)
- OFE copper has excellent thermal conductivity at low temperature.
- A thin (few μm) layer of Nb deposited on a copper cavity \rightarrow decoupling RF - cooling
- LEP2, LHC, HIE ISOLDE cavities were realised with this technology, still actively developed in view of the FCC

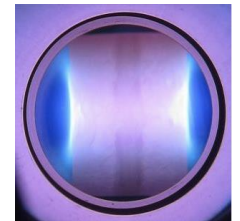


DC magnetron sputtering of 1.3 GHz cavities at CERN

G. Rosaz

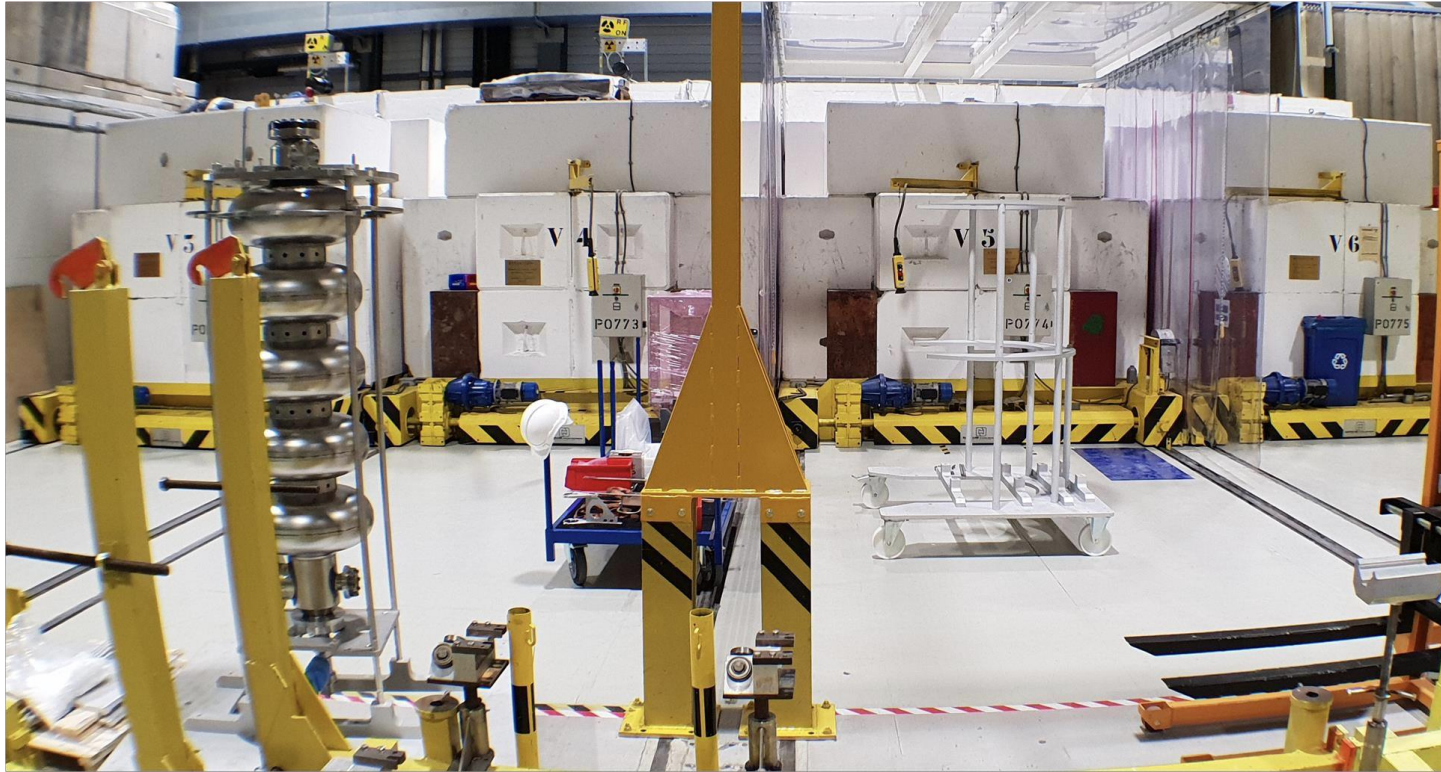


Nb cathode



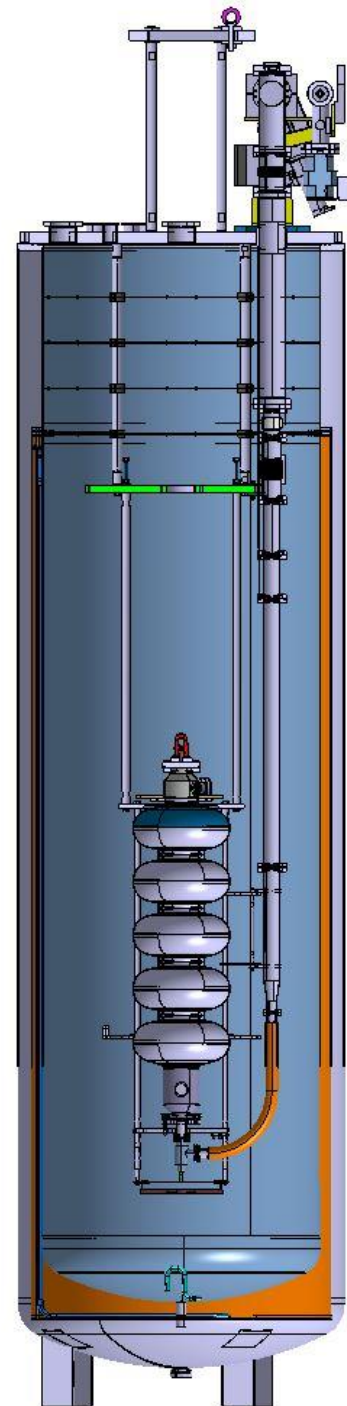
HIPIMS discharge

Cavity testing

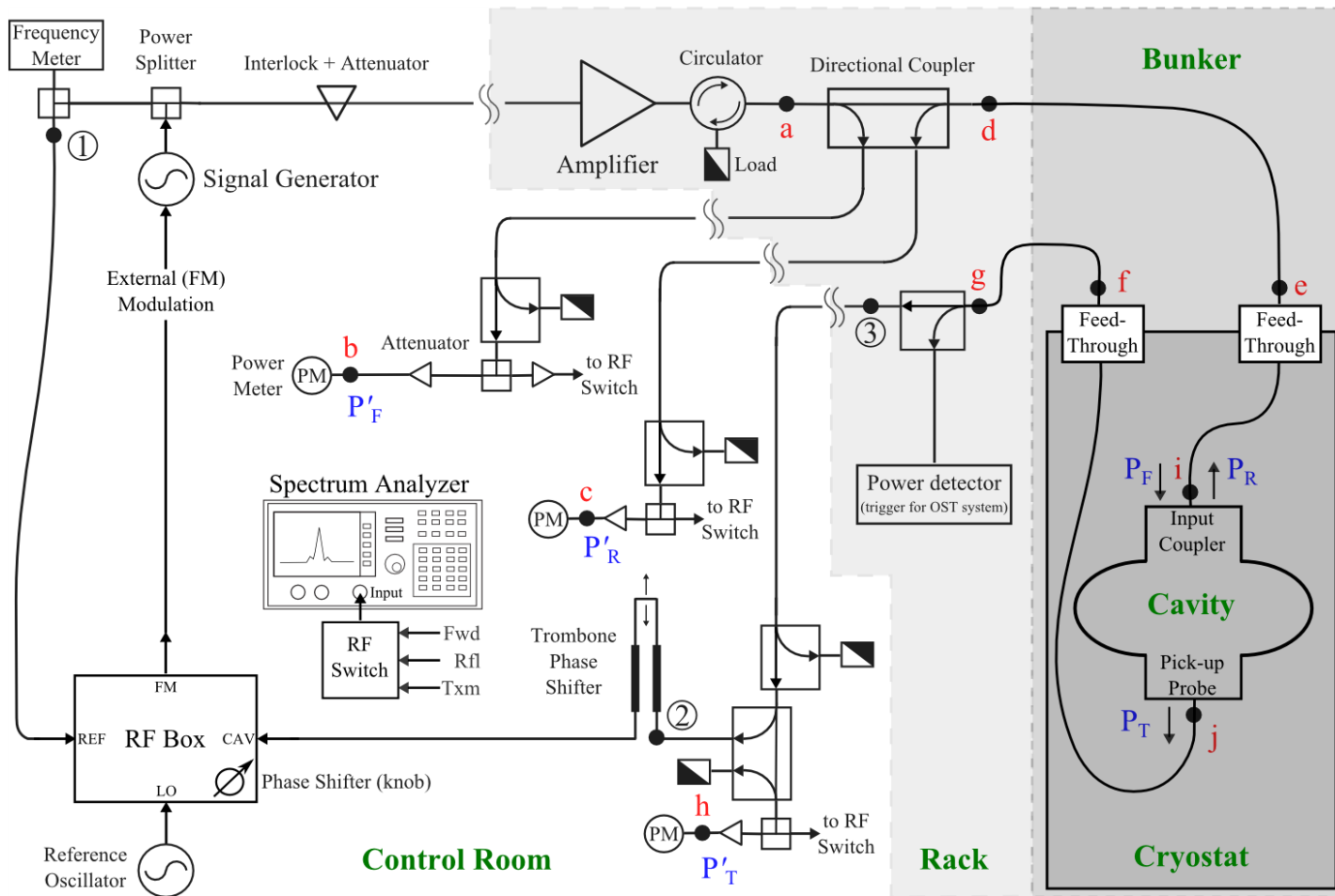


Vertical test area at CERN with bunkers covering 4 cryostat pits.
Liquid helium supplied by valve modules fed by a central cryoplant

Cross section of vertical cryostat with
cavity and pumping line

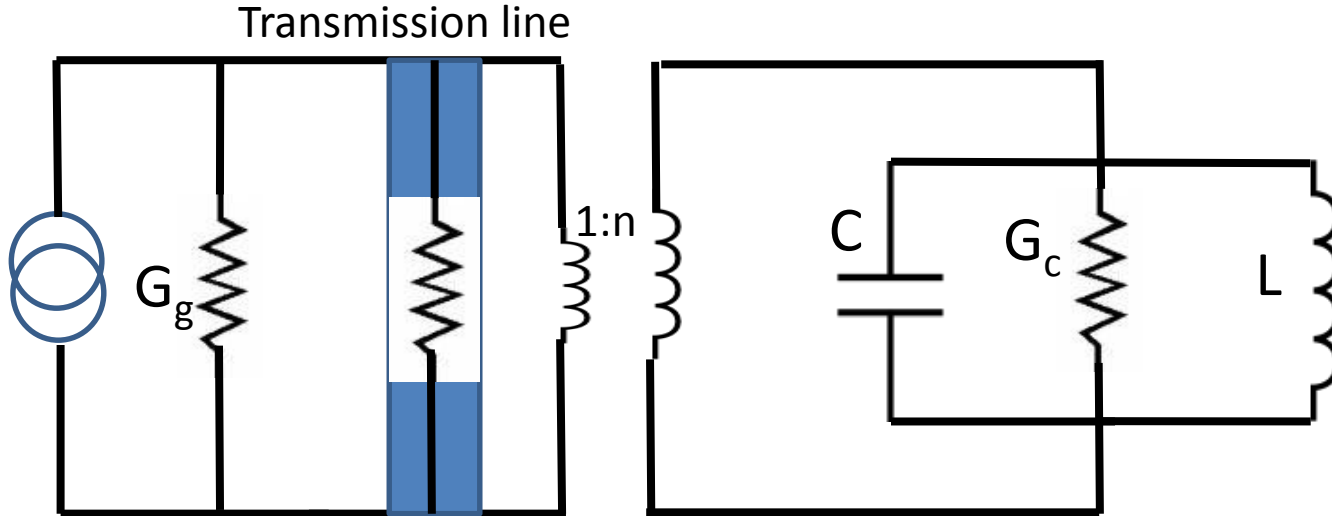


Measurement circuit



Cavity measurement analysis

- Equivalent circuit model (for one mode)



Generator + Circulator

Input Coupler

Cavity

Cavity measurement analysis: undriven cavity:

$$P_{tot} = P_c + P_e + P_t; \rightarrow \text{Loaded Q: } Q_L = \frac{\omega U}{P_{tot}}$$

$$-\frac{dU}{dt} = P_{tot} = \frac{\omega U}{Q_L}; \quad U \text{ decreases exponentially, the time constant is } \tau_L = \frac{Q_L}{\omega}$$

$$\frac{P_{tot}}{\omega U} = \frac{1}{Q_L} = \frac{1}{Q_o} + \frac{1}{Q_e} + \frac{1}{Q_t}; \text{ defines intrinsic and external Q's}$$

$$\text{Coupling parameters: } \beta_e = \frac{Q_o}{Q_e}; \quad \beta_t = \frac{Q_o}{Q_t}$$

they tell how strongly the couplers interact with the cavity.

$$Q_o = Q_L(1 + \beta_e + \beta_t)$$

While external Qs only depend on geometry (overlap of field lines between cavity and coupler), the betas depend on the cavity Q.

Cavity measurement analysis: driven cavity with one coupler

- From the equivalent circuit, the reflection coefficient of the cavity seen from the transmission line can be computed:

- $$\Gamma = \frac{Z_L - Z_0}{Z_L + Z_0} = \frac{1 - \frac{Y_c}{G_0}}{1 + \frac{Y_c}{G_0}}$$

- The conductance seen from the generator, relative to G_0 is $\frac{1}{\beta}$ and the susceptance is $Q_e \left(\frac{\omega}{\omega_0} - \frac{\omega_0}{\omega} \right)$

- Then, the complex reflection coefficient is

- $$\Gamma(\omega) = \frac{\beta - 1 - jQ_0\delta}{\beta + 1 + jQ_0\delta}$$
 and δ is the detuning factor $\delta = \left(\frac{\omega}{\omega_0} - \frac{\omega_0}{\omega} \right)$

- The power flowing in the cavity is $P_{in} = P_f(1 - |\Gamma|^2)$

- The reflected power can be cast in the form $P_r = \left(\sqrt{\frac{\omega_0 U}{Q_e}} - \sqrt{P_f} \right)^2$

- The stored energy obeys the equation:

- $$\frac{d\sqrt{U}}{dt} = \frac{1}{2\tau_L} (\sqrt{U_0} - \sqrt{U}) \quad \rightarrow \quad \frac{dE}{dt} = \frac{1}{2\tau_L} (E_0 - E)$$

Equilibrium value of U
for a given Pf

$$U_0 = \frac{4\tau_L^2 \omega P_f}{Q_e}$$

Cavity behaviour analysis

- Steady state: from the expression of the reflected power $P_r = P_i \left(\frac{\beta-1}{\beta+1}\right)^2$ we

$$\text{derive } \beta = \frac{1 \pm \sqrt{\frac{P_r}{P_i}}}{1 \mp \sqrt{\frac{P_r}{P_i}}}$$

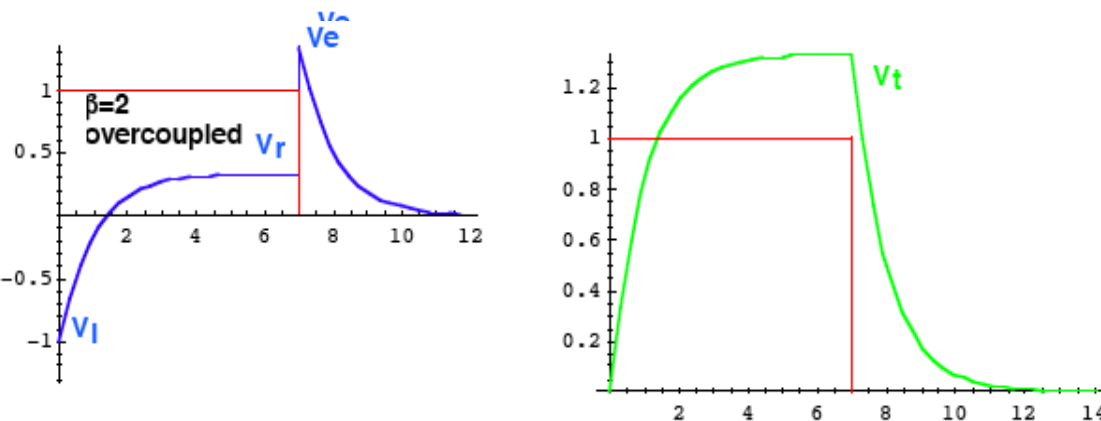
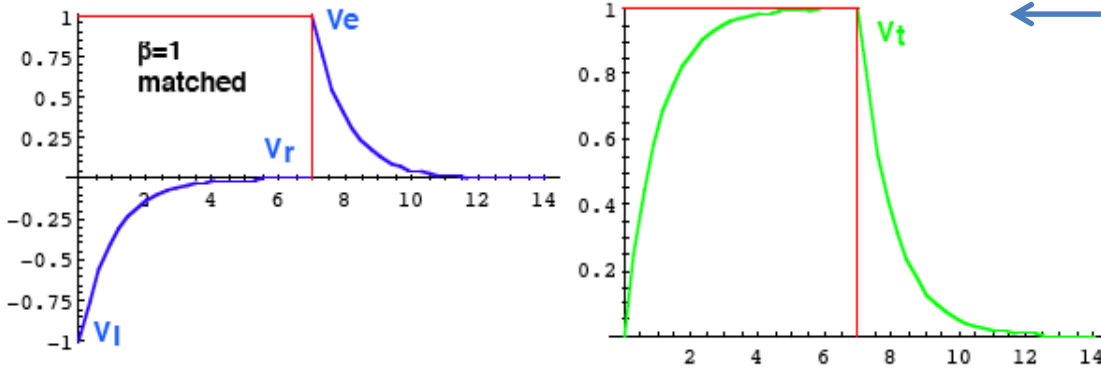
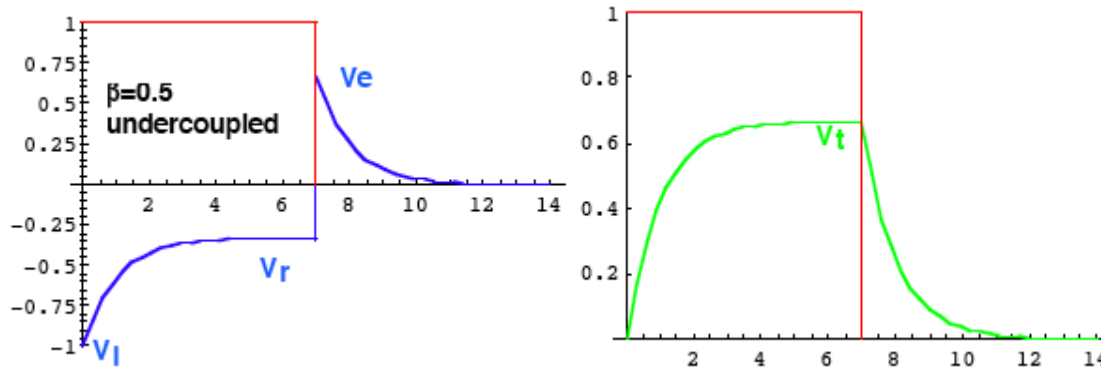
the coupling coefficient is thus determined from the measurement in CW of the reflected and incident power provided it is known if $\beta > 1$ or $\beta < 1$

From the differential equation for E, by setting proper initial conditions, we can analyse the reflected power waveforms at RF turn on and off.

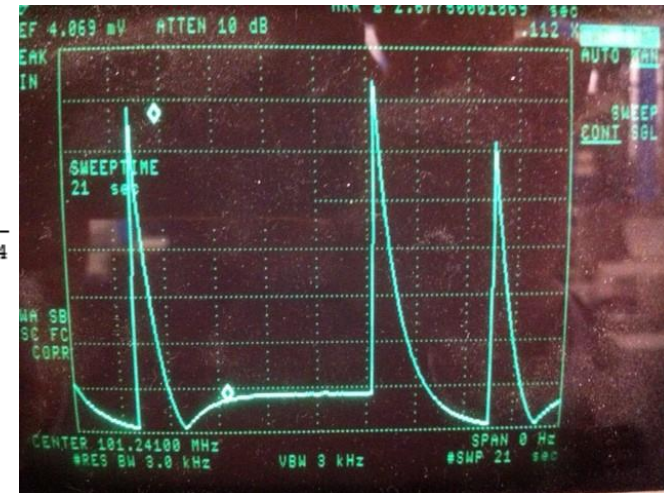
These allow to distinguish the type of coupling

Determination of the coupling factor

$$\beta = \frac{1 - \left| \frac{V_r}{V_i} \right|}{1 + \left| \frac{V_r}{V_i} \right|} = \begin{cases} \frac{|V_i| - |V_r|}{|V_i| + |V_r|}; \beta \leq 1 \\ \frac{|V_i| + |V_r|}{|V_i| - |V_r|}; \beta \geq 1 \end{cases}$$

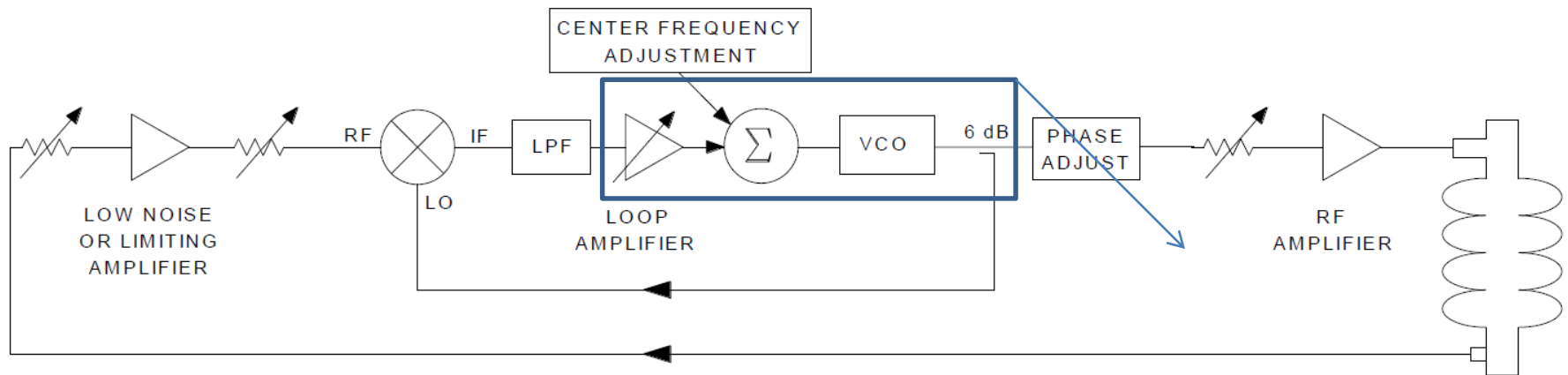


← Voltage waveforms



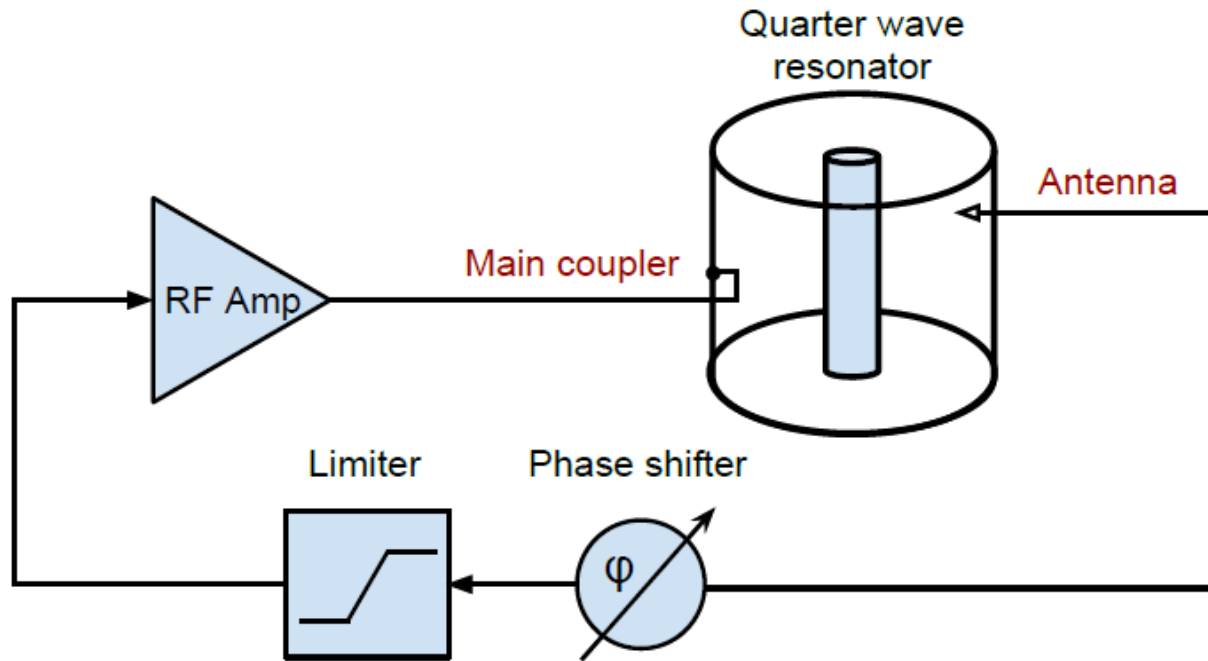
Reflected power from a square pulse when $\beta > 1$

Locking the cavity: generator driven systems



Block diagram of a VCO PLL System. The encircled elements can be replaced by an RF generator which accepts frequency modulation from the DC output of the mixer (phase error-> frequency error around resonance).

Locking the cavity: Self excited loop



High gain, positive feedback loop: the cavity selects its own resonance frequency from the noise floor and the circuits starts to oscillate. Only works with correct phase shift on the return path.

Finds and tracks the cavity resonance

Test stand



Measurement procedure

Calibration point:

- Determine input coupling condition
- Measure in CW: P_i , P_r and P_t
- Measure the time constant of U
- From β and τ_L $Q_0 = \omega_0 \tau_L (1 + \beta)$
- From the measurement in CW, obtain the dissipated power $P_c = P_i - P_r - P_t$
- Find the stored energy by the definition of Q_0 :

$$U_0 = \frac{P_c Q_0}{\omega}$$

- Find the accelerating field $E_{acc} = k_e \sqrt{U_0}$
- Find the calibration constant of the pickup

$$K_{pu} = \frac{U_0}{P_t} = \frac{Q_{ext pu}}{\omega}$$

Q-E scan

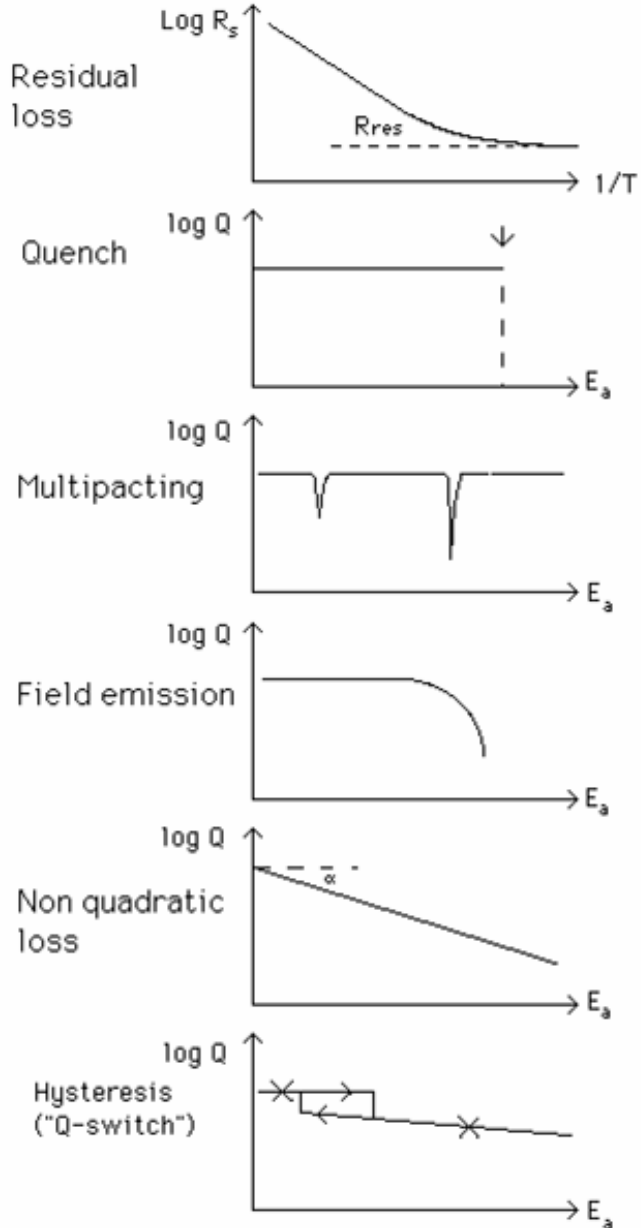
- Increasing the power level, U is determined by the transmitted power, knowing K_{pu} hence the field is determined knowing k_e
- The corresponding value of Q is determined by the definition, knowing the stored energy and the dissipated power



k_e is obtained by means of computer simulations

MP

Interpretation of cavity behaviours



Fitting $Q(T)$ data with the standard BCS expression reveals the so called "non BCS losses"

The global transition of the cavity to the normal conducting state is a catastrophic event, can happen to bulk Nb cavities in case of large beam losses

Multipacting is easily recognized by the "field lock" feature. Also it recurs at the same field levels for the same cavity geometry

Field emission most striking mark is the emission of X rays. The endpoint energy of the spectrum corresponds to the maximum kinetic e^- energy

Many theories available, a lot to understand still

Q switches are small (local) quenches. The cooling power is sufficient to prevent global quench. Typical hysteretic behaviour

Multipacting

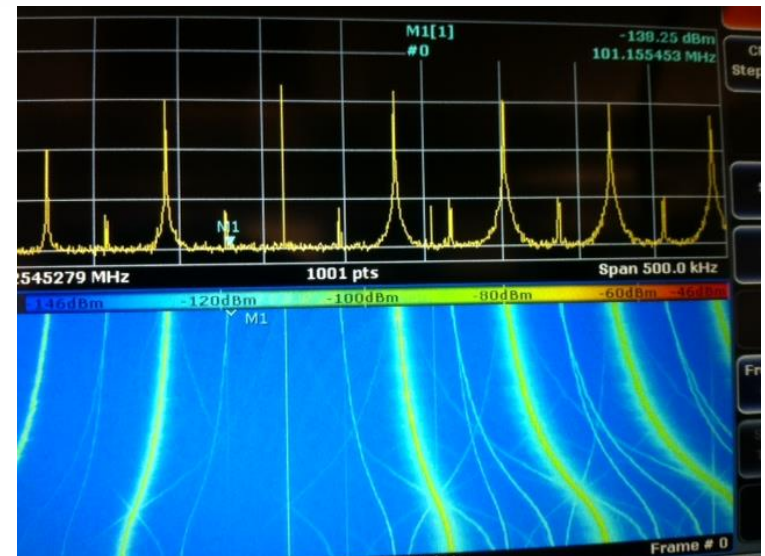
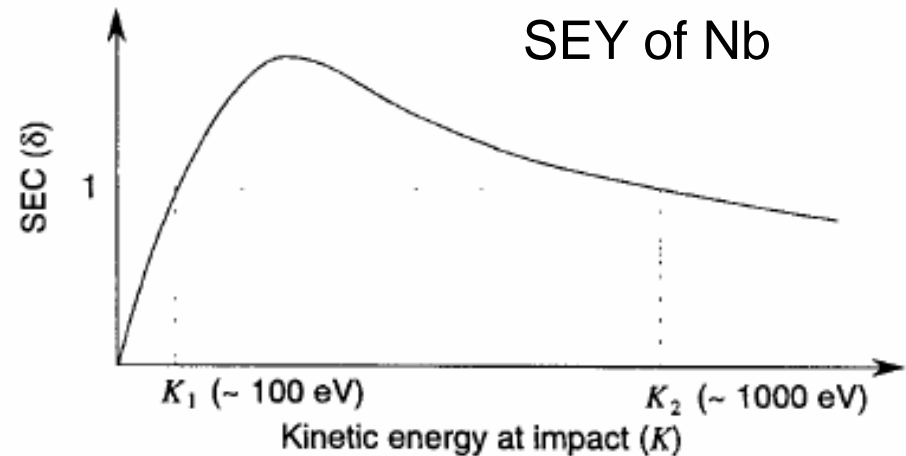
Electron trajectories resonant with RF field

Electrons emitted from the cavity surface are accelerated by E fields, bent by B fields, and strike back the surface (at the same spot or another)

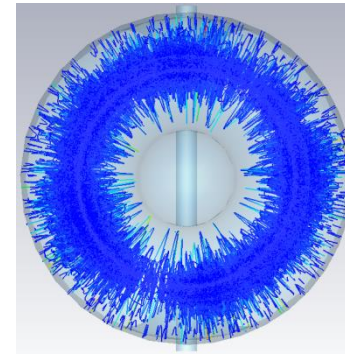
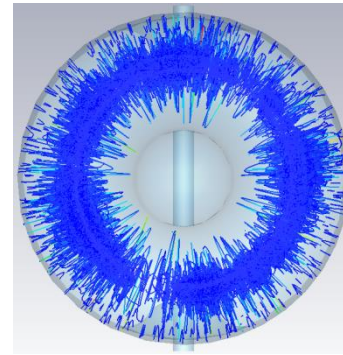
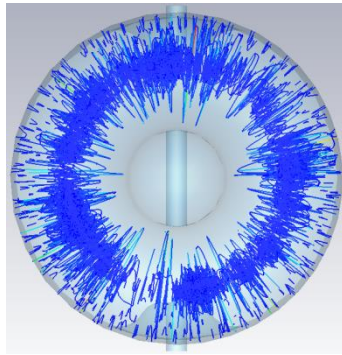
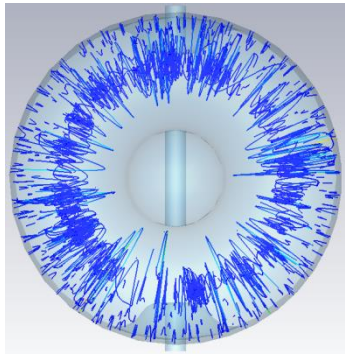
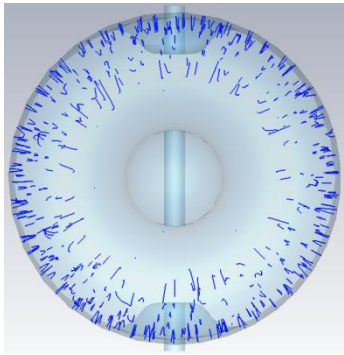
As long as secondary emission yield > 1 , the process restarts with more electrons \rightarrow electron avalanche

RF power is used to sustain exponentially growing electron currents in the cavity, the field cannot increase, is “locked” at the value creating the resonance

In some cases, sidebands appear in the spectrum of the transmitted power, \rightarrow which evolve as the cavity gets conditioned



Multipacting (Cavity Top)

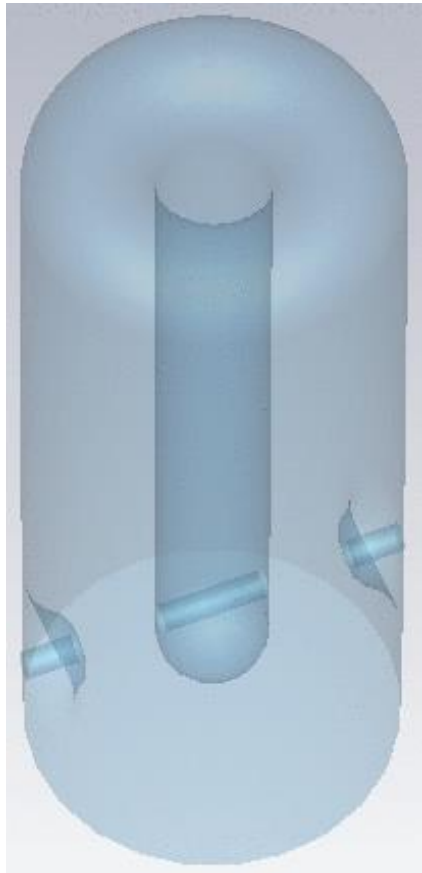


30ns

50ns

70ns

87.5ns



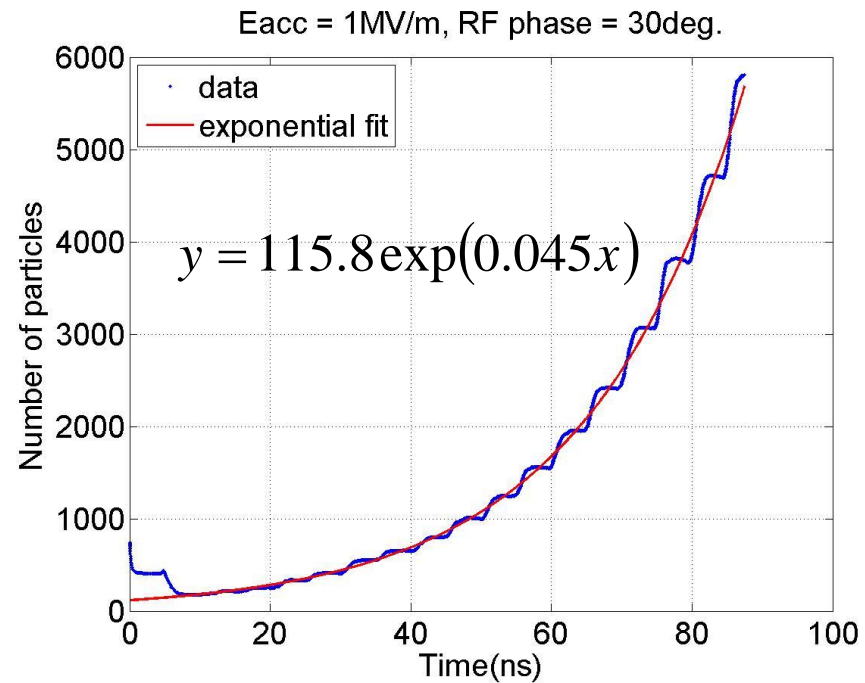
of initial electrons: 742

Kinetic energy: 0-4eV
(uniform)

Emission angle: 0-180 deg.
(random)

Max time steps: 4000

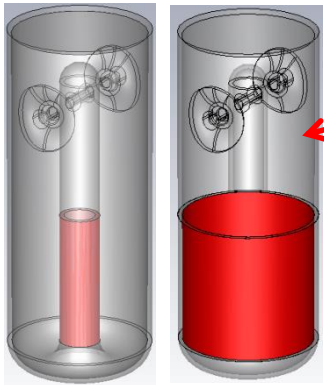
Eacc=1MV/m (30 deg)



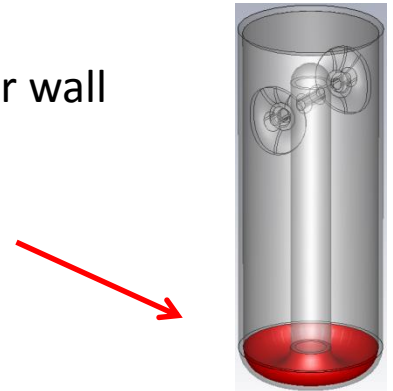
Multipacting Summary

■ Antenna ■ Outer wall

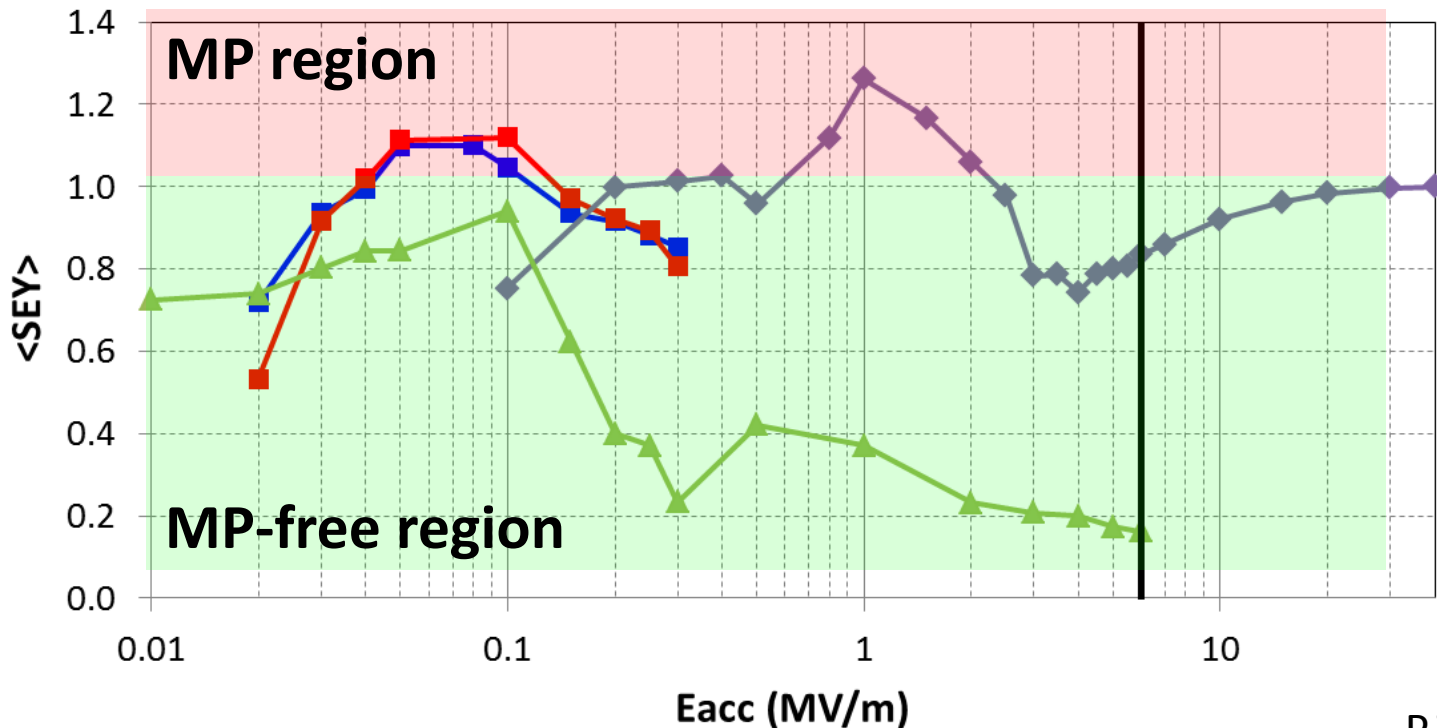
◆ Cavity top



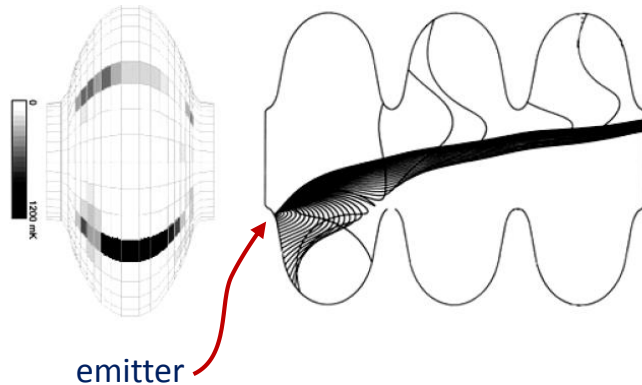
- MP happens at low fields for antenna region and outer wall
 - $E_{acc} = 0.05-0.1 \text{ MV/m}$
- MP happens at higher fields for cavity top region
 - $E_{acc} = 0.8-2 \text{ MV/m}$



■ Antenna ■ Outer wall ◆ Cavity top ▲ Antenna tip — Eacc=6MV/m



Field emission: Fowler-Nordheim theory



FE current

FE current density

$$I(E) = j(E)A_e \quad j(E) = \frac{A_{FN}(\beta_{FN}E)^2}{\Phi} \exp\left(-\frac{B_{FN}\Phi^{3/2}}{\beta_{FN}E}\right)$$

A_{FN}, B_{FN} constants

Φ work function of the metal

E instantaneous electric field

A_e field emitter area

b_{FN} field enhancement factor correcting E

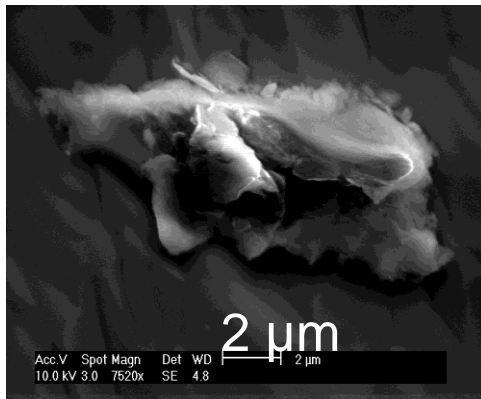
Large range of b and A_e

Work function barrier at the surface is lowered by applied electric field, so electrons tunnel through it. F-N needs correction by “field enhancement factor” related to emitter’s physical properties

Emitters are most likely metals, 100/cm², 0.3-20mm

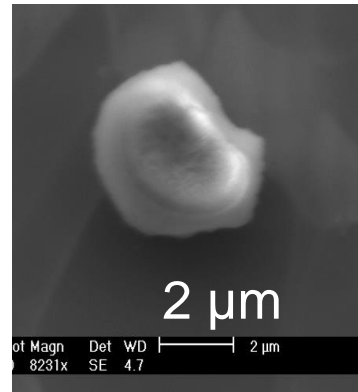
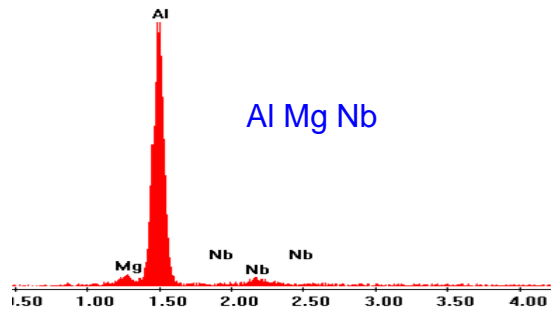
Irregular shape enhances FE.
Interface to substrate is relevant: condensed gas contribute to “activate” contaminant particulates as field emitters, enhancing tunneling probability
R.L.Geng THOBB031 IPAC2016

- Typical particulate emitters



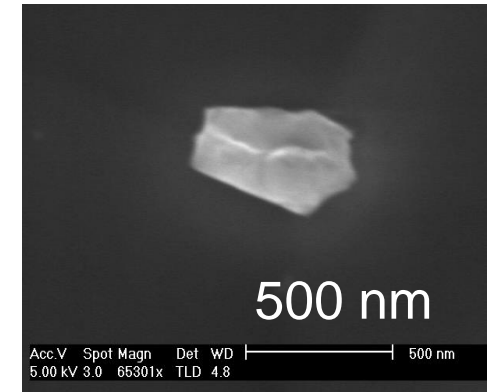
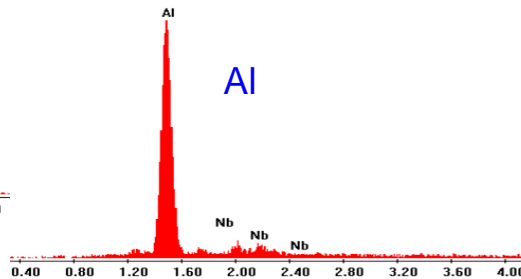
$$E_{on}(2nA) = 140 \text{ MV/m}$$

$$\beta = 31, S = 6.8 \cdot 10^{-6} \mu\text{m}^2$$



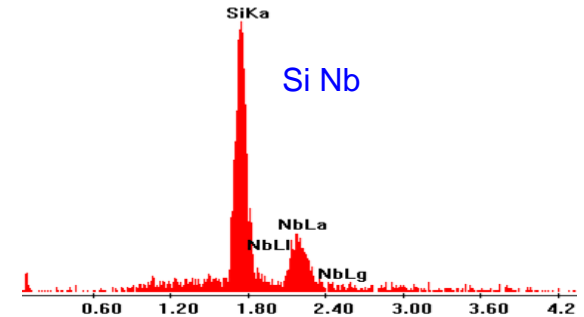
$$E_{on}(2nA) = 132 \text{ MV/m}$$

$$\beta = 27, S = 7 \cdot 10^{-5} \mu\text{m}^2$$

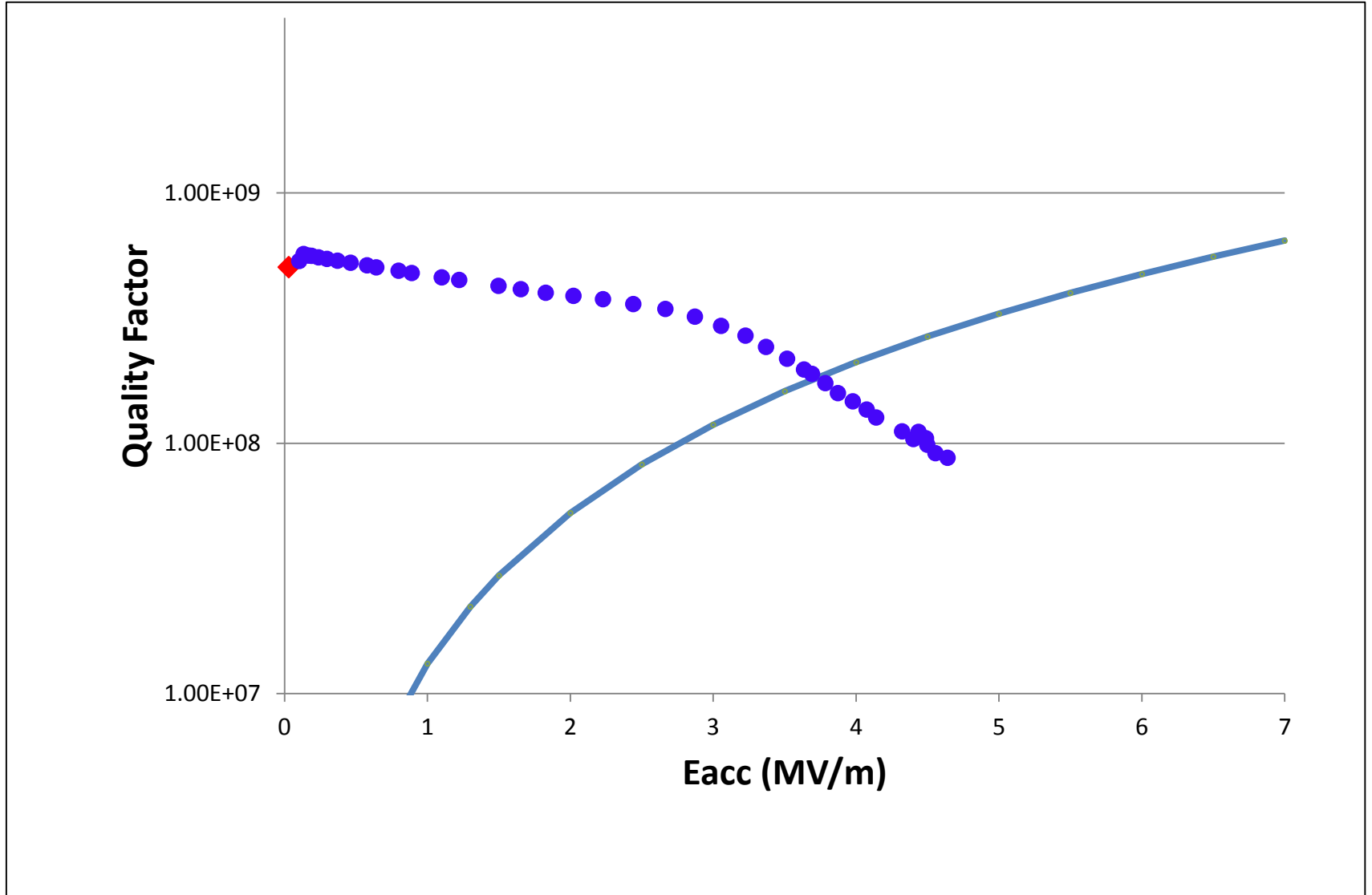


$$E_{on}(2nA) > 120 \text{ MV/m}$$

$$\beta = 46, S = 6 \cdot 10^{-7} \mu\text{m}^2$$



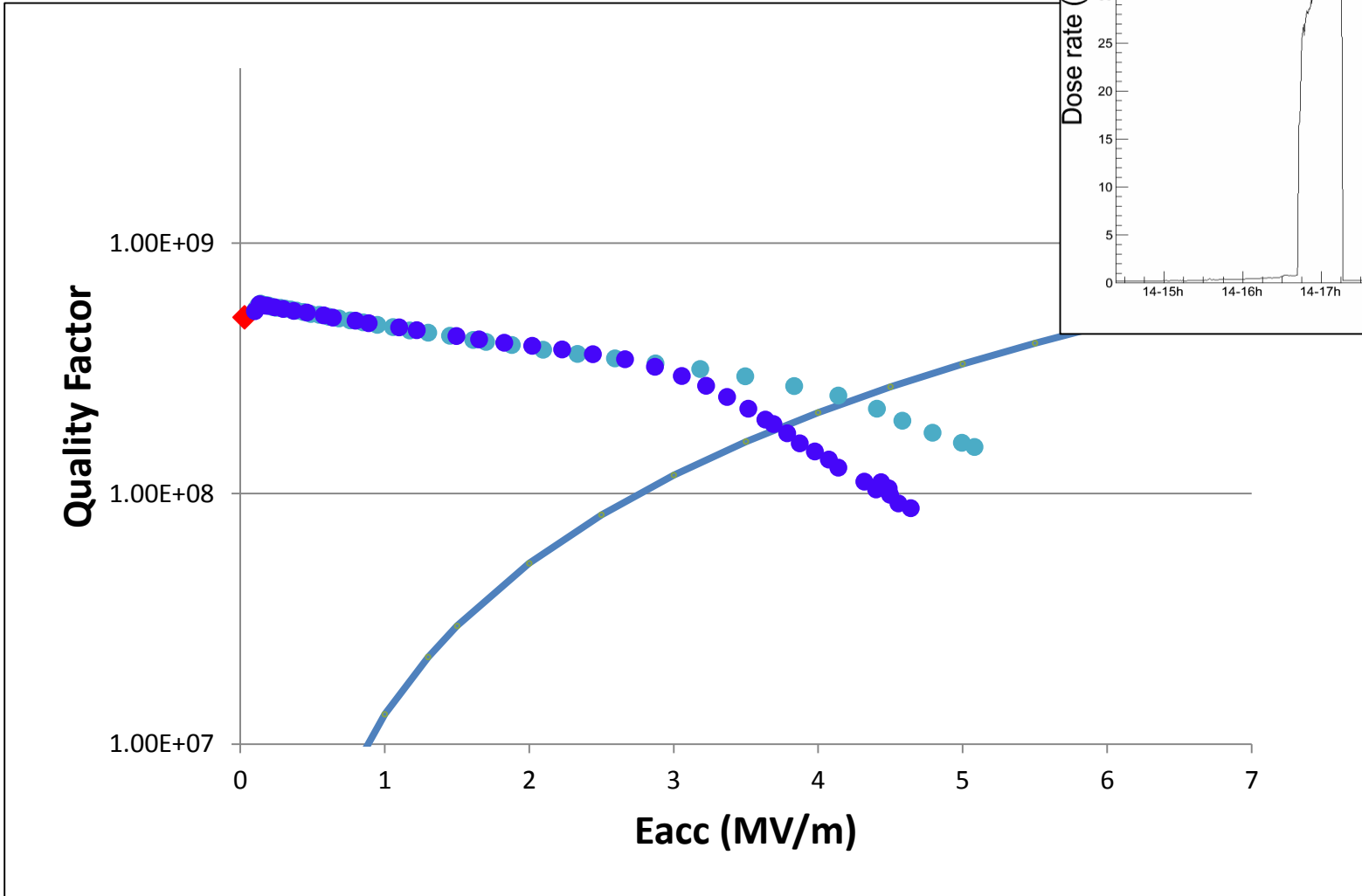
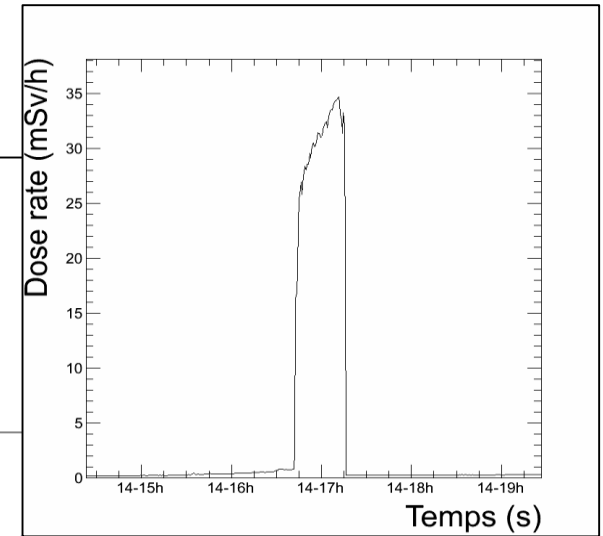
Field Emission in Q-E curve



He processing

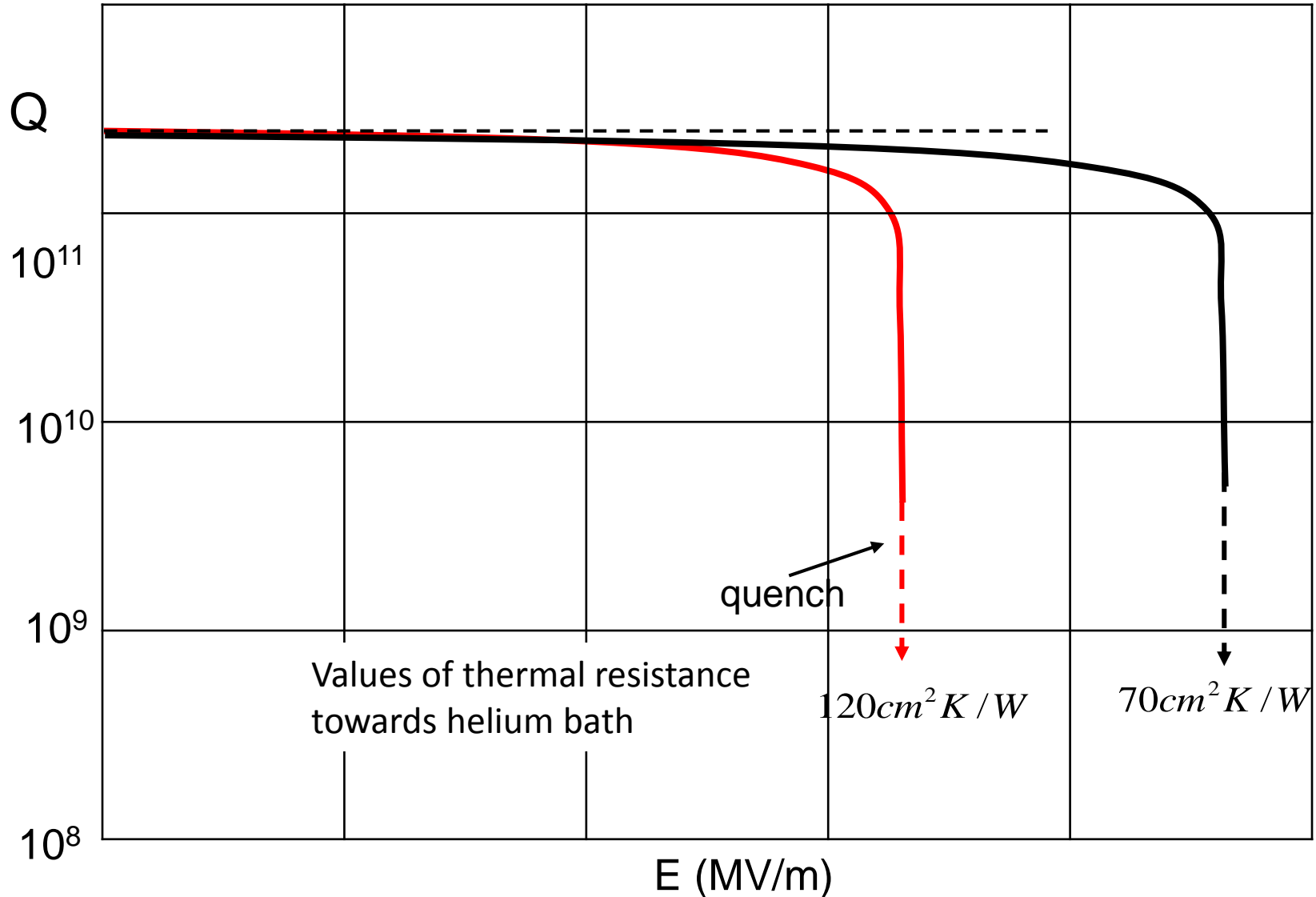
- Low pressure helium gas injected in cavity vacuum
- Supplying RF power, gas ionization occurs and a low density plasma is generated, which can “clean” emitters

Dose rate data



Global thermal instability

Poor cooling conditions with positive feedback due to R_{BCS} exponential temperature dependence may lead to cavity quench



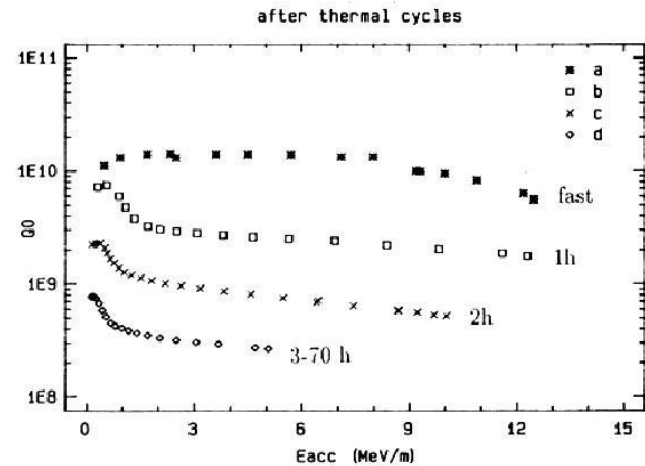
Q disease

Hydrides segregation during cool down

Slow cool down around 100 K is detrimental

Cured by H outgassing in vacuum at elevated temperature

According to a recent theory nano hydrides may be responsible for high field Q slope



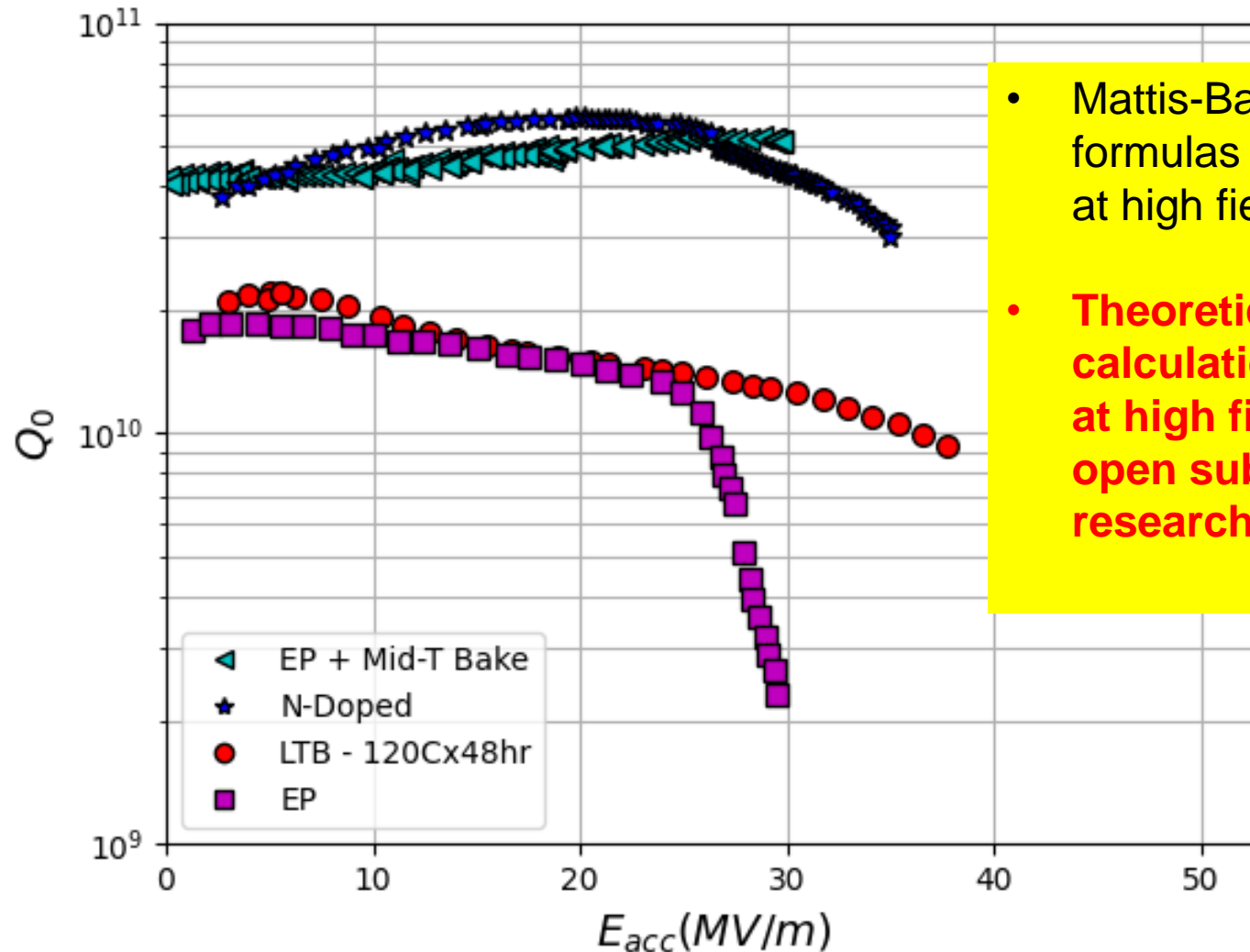
B. Bonin and R. W. Roth, Proc. 5th SRF Workshop, Hamburg,



F. Barkov, A. Romanenko, and A. Grassellino, Phys. Rev. ST Accel. Beams 15, 122001 (2012)

Field dependent surface resistance

- Diverse behaviours of $R_s(H)$ observed experimentally, depending on surface treatments modifying the RF layer.



- Mattis-Bardeen formulas do not apply at high field
- **Theoretical calculations of R_{BCS} at high field still an open subject of research.**